Experimental Characterization of Ranging in IEEE802.15.4a using a Coherent Reference Receiver

Thomas Gigl†‡, Josef Preishuber-Pfluegl‡, Daniel Arnitz†, and Klaus Witrisal†

{thomas.gigl, daniel.arnitz, witrisal}@tugraz.at, j.preishuber-pfluegl@cisc.at
†Signal Processing and Speech Communication Laboratory, Graz University of Technology, Austria
‡CISC Semiconductor, Design and Consulting GmbH, Austria

***Abstract*—Real time locating systems (RTLS) and wireless sensor networks are currently a hot and challenging research topic. Ultra wideband (UWB) shows promising properties for these systems, such as low-power transmitter designs and highly accurate ranging, where cm-level accuracy is achievable even in multipath intensive environments. A high-performance reference receiver architecture based on coherent processing is presented in this paper. It is used to define quality metrics of the received signals, as for example peak signal to noise ratio (PSNR) and line-of-sight signal to noise ratio (LSNR) for ranging, and *Eb/N0* for communication. These metrics are used to evaluate the experimental data in their quality and their ranging performance. Furthermore, performance trade-offs w.r.t. system parameter and receiver architecture choices, in particular for non-coherent receivers, can be analyzed. In this work, the reference receiver is verified experimentally using IEEE 802.15.4a compliant signals. The ranging performance is correlated to the signal-to-noise ratios for an indoor line-of-sight measurement campaign.**

I. Introduction

The IEEE 802.15.4a standard [1] describes a low-complexity wireless sensor network with sub-meter localization accuracy. The physical layer, which is specifically designed for ranging, is a UWB impulse radio transmission scheme with bi-directional communication. The application of coherent and non-coherent receiver architectures is possible. Coherent receiver architectures show high complexity due to high sampling rates and accurate synchronization requirements. Sub-optimum non-coherent receiver architectures can drastically reduce this complexity, at the cost of some performance loss [2]. Sub-Nyquist sampling is applicable, but limits the ranging accuracy. Several non-coherent receiver architectures have been tested and compared by simulations (e.g., [3]), and experiments, (e.g., [4] [5]).

The presented coherent receiver architecture is specifically designed for synchronized experimental setups and high performance. The coherent receiver can be used as a performance benchmark for ranging and communication in comparison to other, less complex, receiver architectures. In this work, the receiver is used to quantify the quality of indoor Line-Of-Sight (LOS) measurements by defining different signal-to-noise ratios and analyzing their influence on the ranging accuracy.

The rest of the paper is organized as follows: Section II gives an overview of the introduced receiver architecture, while Section III presents the mathematical signal model. The used ranging algorithm is presented in Section IV. A statistical analysis of the receiver and the definition of specific performance metrics for ranging and communication are given in Section V. In Section VI, the receiver is verified in an indoor LOS scenario and finally, Section VII sums up the results.

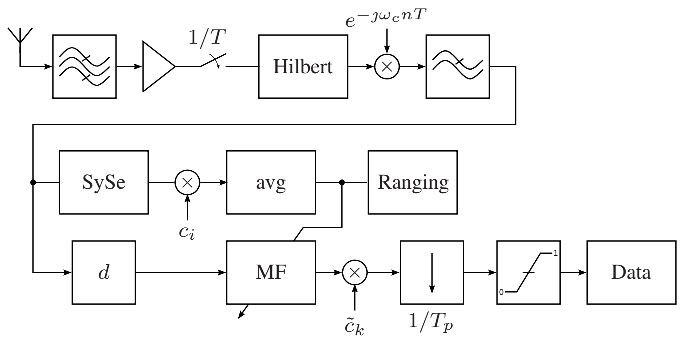

Fig. 1: Coherent receiver architecture

II. System model

The proposed reference receiver architecture is shown in Fig. 1. The receiver is assumed to be synchronized, thus the timing is known, which is easily achieved in an experimental setup. The signal is received by a UWB antenna, amplified by a low noise amplifier and sampled by a real-time scope. The negative spectrum parts are removed by a Hilbert filter and the signal is down-converted to baseband by multiplication with the carrier frequency. A lowpass filter reduces the out-of-band noise in the input signal. Next, the signal is divided into a matched-filter estimation path (upper signal path) and a communication path (lower signal path). The receiver is assumed to be synchronized, thus a code frame separation is applied in the Synchronized Separation (SySe) block. Next, code despreading is performed to enhance the SNR and to cancel inter-pulse interference. Finally, the channel estimation is done by averaging over the received despread pulse frames, yielding the channel estimate for the matched-filter (MF) (see Section III). The ranging algorithm is performed directly on the channel estimate, see Section IV. The lower part of the receiver is used for communication and is implemented as a well known matched filter structure. The delay d is required to account for the processing time of the MF estimation. Next, the code despreading is performed. Its output is downsampled to the symbol rate for communications. The next chapter gives a detailed description of the receiver, based on a signal model.

III. Signal Model

The following notations are used: Column vectors and matrices are denoted by lower and upper-case boldface symbols, respectively. Estimated values are marked by hats.

The preamble symbol $\mathbf{c}_s$ is designed compliant to the IEEE 802.15.4a standard and has a symbol length N_s of 31 or 127. It consists of ternary elements $\in \{-1, 0, 1\}$. The spread preamble code vector $\mathbf{c}_{sp}$ is created as

$$\mathbf{c}_{sp} = \mathbf{1}_{N_{pr}} \otimes \mathbf{c}_s \otimes \mathbf{u}_L = \mathbf{c} \otimes \mathbf{u}_L \tag{1}$$

where $\mathbf{1}_{N_{pr}}$ is a vector of ones with length N_{pr}, $\otimes$ denotes the Kronecker product, $\mathbf{u}_L$ is the spreading sequence of the preamble, which is defined as a unit vector with an one at the first position and length L. The transmitted signal $s(t)$ is defined as

$$s(t) = \mathrm{Re}\{s_l(t)e^{j\omega_c t}\} = \mathrm{Re}\left\{\sum_{m=0}^{M-1} c_m w(t - mT_c)e^{j\omega_c t}\right\} \tag{2}$$

where $\mathrm{Re}\{.\}$ is the real operator, $s_l(t)$ is the baseband signal, c_m is the m-th element of $\mathbf{c}$, $w(t)$ is the pulse shape, M is the number of code frames in the preamble and ω_c is the carrier frequency. A code frame is the duration of the pulse repetition period in the sprea preamble $T_c = LT_{chip}$, where T_{chip} is the chip repetition period. The transmitted signal is sent over a multipath channel with channel impulse response $h_c(t)$. The effects of the antennas and the frontend filter are contained in the channel for simplicity. Thus, the analog received signal $r_a(t)$ can be described as

$$r_a(t) = s(t) * h_c(t) + \nu(t) \tag{3}$$

where $\nu(t)$ is modeled as additive white Gaussian noise and $*$ is the convolution. The analog input signal is sampled by $1/T$, thus the discrete time signal is defined by $r_a[n]{=}r_a(nT)$. Next, the negative frequencies are canceled by a Hilbert filter $h_{hilb}[n]$ and the complex baseband signal is obtained by down-converting the signal with the estimated carrier frequency $\hat{\omega}_c$. The resulting digital baseband signal is

$$\begin{aligned} r[n] &= \left\{(r_a[n] * h_{hilb}[n])\, e^{-j\hat{\omega}_c nT}\right\} * h_{LP}[n] \\ &= \sum_{m=0}^{M-1} c_m h(nT - mT_c)e^{j[\omega_c - \hat{\omega}_c]nT} + \nu_l[n] \end{aligned} \tag{4}$$

where $h(t)$ is an equivalent channel response incorporating the pulse $w(t)$, the channel $h_c(t)$ and the lowpass filter $h_{LP}[n]$. The filter $h_{LP}[n]$ is implemented to reduce the noise energy in the received signal and has a gain of one in the passband. The noise $\nu_l[n]$ is the band limited input noise $\nu_l[n]{=}\nu[n] * h_{LP}[n]$, where $\nu[n]$ is assumed to be white Gaussian with variance σ_n^2, because of the much smaller bandwidth of $h_{LP}[n]$ in comparison to the frontend filter. The carrier is hardware locked in the experiments, thus its frequency is known and (4) simplifies to

$$r[n] = \sum_{m=0}^{M-1} c_m h[n - mN_c] + \nu_l[n] \tag{5}$$

where $h[n]{=}h(nT)$. The number of samples in a code frame is defined by $N_c{=}T_c/T$. Due to synchronization the code frames can be separated by the following method: A matrix $\mathbf{R}$ with dimensions $N_{\hat{h}} \times M$ is defined. $N_{\hat{h}}$ is the length of the matched filter and should be chosen such that the maximum excess delay of the channel is included. Note that inter-pulse-interference (IPI) can occur, i.e., $N_{\hat{h}}$ can be greater than N_c. $\mathbf{R}$ is filled by $R_{a,b}{=}r[a + bN_c]$, where the channel impulse responses will partly overlap in the columns if $N_{\hat{h}}{>}N_c$. The estimation of the channel response is performed by

$$\hat{\mathbf{h}} = \frac{\mathbf{R}\,\mathbf{c}}{M_1}\ . \tag{6}$$

Only the non-zero coded signals account in this equation, thus the number of non-zero coded pulses is taken into account by $M_1{=}(M + N_{pr})/2$. IPI cancels by despreading due to the perfect autocorrelation properties of the code, hence the observed multipath components are well reconstructed. A detailed analysis of the estimation of $h[n]$ will be given in the next section.

IV. Ranging Algorithm

The detection of the LOS component for range estimation is implemented as a search back algorithm using the samples $\hat{h}[n]$ of the estimated channel response $|\hat{\mathbf{h}}|$. This is written as

$$\hat{\tau}_{los} = \min\{n|\ |\hat{h}[n]| \geq \gamma\}\, T \tag{7}$$

where $\hat{\tau}_{los}$ is the delay of the LOS component, w.r.t. the synchronization time $t{=}0$, which is given by the experimental setup. γ is a threshold, which is defined as [6]

$$\gamma = \bar{\nu}_{\hat{h}} + c(\hat{h}_{\max} - \bar{\nu}_{\hat{h}}) \tag{8}$$

where the peak value $\hat{h}_{max}{=}\max\{|\hat{h}[n]|\}$ is used as reference value for the threshold detection, $\bar{\nu}_{\hat{h}}$ is the mean magnitude of the noise in $\hat{h}[n]$, and $0{<}c{\leq}1$ is a user-defined threshold, where $c = 1$ implements peak detection. The noise is assumed to be zero-mean circularly symmetric complex Gaussian. Therefore the, mean magnitude $\bar{\nu}_{\hat{h}}$ of the complex noise samples is given by the expected value of a Rayleigh distribution, which is related to the sample variance by

$$\bar{\nu}_{\hat{h}} = \mathrm{E}\{|\nu_{\hat{h}}|\} = \sqrt{\frac{\pi}{4}\sigma^2_{\hat{h}[n]}} \tag{9}$$

Note, that a search back algorithm with fixed window size [7] can be also implemented, if the necessary data is provided to the algorithm, which means that the synchronization time is shifted according to the window length.

V. Statistical Analysis

This section defines the performance metrics of the coherent receiver. E_b/N_0 of a matched filter is a well-defined performance metric in communications and is thus used as reference, where E_b is the energy per bit and N_0 is the noise spectral density. First, the ranging and MF estimation path are analyzed in detail.

A. Estimation of $\mathbf{h}$

Equation (6) can be re-written with (5) to

$$\hat{h}[n] = \frac{1}{M_1}\sum_{m=0}^{M-1} c_m^2\, h[n] + c_m \nu_l[n+mN_c] \quad . \tag{10}$$

As mentioned in Section III, only the non-zero coded signals show an influence on the estimation of $\mathbf{h}$, thus the averaging is only done with these symbols.

1) Expected value of $\hat{h}[n]$: The expected value of $\hat{h}[n]$ is given by

$$\mathrm{E}\Big\{\hat{h}[n]\Big\} = \frac{1}{M_1}\sum_{m=0}^{M-1} c_m^2 h[n] = h[n] \tag{11}$$

where only the deterministic part of the signal counts, due to the zero mean noise.

2) Variance of $\hat{h}[n]$: The variance of $\hat{h}[n]$ is defined by the variance of the noise component in (10) and is given by

$$\begin{aligned}\mathrm{var}\Big\{\hat{h}[n]\Big\} =& \frac{1}{M_1^2}\sum_{m=0}^{M-1}\sum_{v=0}^{M-1} c_m c_v \\ & \times \mathrm{E}\{\nu_l[n+mN_c]\nu_l^*[n+vN_c]\} \\ =& \frac{1}{M_1^2}\sum_{m=0}^{M-1}\sum_{v=0}^{M-1} c_m c_v R_{\nu_l}[(m-v)N_c]\end{aligned} \tag{12}$$

where $R_{\nu_l}[k]$ is the autocorrelation function of $\nu_l[n]$. Therefore, we get

$$\mathrm{var}\Big\{\hat{h}[n]\Big\} = \frac{1}{M_1^2}\sum_{m=0}^{M_1-1} c_m^2 R_{\nu_l}[0] \tag{13}$$

because noise samples spaced by $\geq\ N_c$ are uncorrelated, $R_{\nu_l}[k]{=}0$ for $k{\geq}N_c$. Furthermore, we can write $R_{\nu_l}[0]{=}\sigma_n^2\phi_{LP}$, where σ_n^2 is the variance of a white noise process and $\phi_{LP}{=}\sum_{n=-\infty}^{\infty}|h_{LP}[n]|^2$ is the equivalent bandwidth of the low pass filter. Thus, the variance is given by

$$\mathrm{var}\Big\{\hat{h}[n]\Big\} = \frac{1}{M_1}\sigma_n^2\phi_{LP} \tag{14}$$

which shows a reduction of the noise by $1/M_1$ and influence of the lowpass filter

B. Derivation of E_p/N_0

The E_b/N_0 is a valuable performance metric in digital communications, because it is independent of the actual waveform of the received signal. A similar measure is proposed as a reference Signal to Noise Ratio (SNR) for ranging, which relates E_p, the total energy in the preamble signal, to N_0. To obtain E_p/N_0, the matched filter output is analyzed, which is written

$$\mathbf{y} = \mathrm{Re}\Big\{\mathbf{R}^H\hat{\mathbf{h}}\Big\} \quad . \tag{15}$$

The vector $\mathbf{y}$ contains the receive pulse energies, IPI and noise. Re$\{.\}$ cancels the imaginary noise terms after matched filtering. $\mathbf{R}^H$ is the Hermitian of $\mathbf{R}$. After code despreading IPI cancels again and the matched filter output for the whole preamble is given by $z = \mathbf{y}^T\,\mathbf{c}$,

$$z = \mathrm{Re}\left\{\sum_{m=0}^{M-1}\sum_{n=0}^{N_{\hat{h}}-1} c_m^2 h^*[n]\hat{h}[n] + c_m\nu_l^*[n+mN_c]\hat{h}[n]\right\} \tag{16}$$

where * denotes the complex conjugate. Analyzing mean and variance of z relates the signal model to E_p/N_0.

1) Expected value of z: Since the noise is zero-mean, the mean value E$\{z\}$ is written as

$$\mathrm{E}\{z\} = \mathrm{Re}\left\{\sum_{m=0}^{M-1}\sum_{n=0}^{N_{\hat{h}}-1} c_m^2 h^*[n]\hat{h}[n]\right\} \approx M_1 E_h = E_p \tag{17}$$

E_h is the energy of $h[n]$ and E_p is the preamble energy.

2) Variance of z: The output noise of the matched filter is obtained by $\nu_{MF}[n]{=}\nu[n]{*}h_{LP}[n]{*}h_{MF}[n]$. The impulse response of the matched filter is given by $h_{MF}[n]{=}\hat{h}[N_{\hat{h}}-n]$. We assume that the lowpass filter passes the matched filter without introducing any gain or distortion. Assuming a linear phase of an FIR lowpass filter, it follows that $h_{LP}[n]{*}h_{MF}[n]{=}h_{MF}[n+N_{LP}]$. For simplicity, the additional delay N_{LP} is dropped in the further derivation. The variance of z is calculated similar to the variance of $\hat{h}[n]$,

$$\begin{aligned}\mathrm{var}\{z\} =& \frac{1}{2}\sum_{m=0}^{M-1}\sum_{v=0}^{M-1}\sum_{n=0}^{N_{\hat{h}}-1}\sum_{u=0}^{N_{\hat{h}}-1} c_m c_v \hat{h}[n]\hat{h}^*[u] \\ & \times \mathrm{E}\{\nu[n+mN_c]\nu^*[u+vN_c]\}\end{aligned} \tag{18}$$

where $1/2$ accounts for the Re$\{.\}$. Due to the correlation properties of the code and the additive white Gaussian noise (AWGN), we can reduce the summation to the cases $m{=}v$ and $n{=}u$. It follows, that

$$\mathrm{var}\{z\} = \frac{1}{2}M_1\,\sigma_n^2\,E_h = \frac{1}{2}\sigma_n^2 E_p \tag{19}$$

With (17) and (19), the SNR is defined by

$$\frac{\mathrm{E}^2\{z\}}{\mathrm{var}\{z\}} = \frac{2E_p}{\sigma_n^2} = \frac{2E_p}{N_0} \tag{20}$$

It follows that $\sigma_n^2{=}N_0$ and $(E_p/N_0)_{\mathrm{dB}}{=}10\log(E_p/N_0)$. E_p/N_0 is related to $\sigma^2_{\hat{h}[n]}$ by (20) and (14):

$$\sigma^2_{\hat{h}[n]} = \frac{1}{M_1}\sigma_n^2\phi_{LP} = E_h\phi_{LP}\left(\frac{E_p}{N_0}\right)^{-1} \tag{21}$$

E_p/N_0 does not account for the shape of the channel response $\hat{h}[n]$, which is practicable for communications but not for ranging. Thus, other performance metrics are needed for comparison with respect to ranging.

C. Performance Metrics for Ranging

1) Peak Signal-to-Noise-Ratio: A typical ranging performance metric is the peak signal to noise ratio (PSNR), which is defined as follows [6]:

$$\text{PSNR}_{\text{dB}} = 10\log\left(\frac{\hat{h}^2_{max}}{\sigma^2_{\hat{h}[n]}}\right) = 10\log\left(\frac{\hat{h}^2_{max}}{E_h\phi_{LP}}\frac{E_p}{N_0}\right) \quad (22)$$

It can be observed that this metric depends on the ratio of peak power of the impulse response to the total energy of the pulse response and the low pass filter bandwidth ϕ_{LP}. Many ranging algorithms use the maximum signal component as reference for line of sight detection and/or threshold calculation, e.g., [6], [7]. It can be expected that this performance measure correlates well with the ranging error. On the other hand, the major goal in ranging is the detection of the LOS component, which is not always the strongest component [3]. Thus, the LOS SNR is needed.

2) Line-of-Sight Signal-to-Noise-Ratio: The LOS performance metric is defined as

$$\text{LSNR}_{\text{dB}} = 10\log\left(\frac{|h_l|^2}{\sigma^2_{\hat{h}[n]}}\right) = 10\log\left(\frac{|h_l|^2}{E_h\phi_{LP}}\frac{E_p}{N_0}\right) \quad (23)$$

where h_l is the amplitude of the LOS component in $\hat{\mathbf{h}}$. The advantage of this value is the involvement of the LOS component, which directly defines the performance of the ranging algorithm.

D. Estimation of N_0

The output of z is a scalar, thus it cannot be used to estimate var$\{z\}$ for one specific measurement. The preamble symbols are used instead. For that purpose, the code despreading is done per preamble symbol. The matrix $\mathbf{Y}_s$ is created and has the dimensions $N_s \times N_{pr}$. It is filled by $\mathbf{Y}_{s;a,b} = y[a + bN_s]$. The despread code symbols are given by

$$\mathbf{z}_s = \mathbf{Y}_s^T \mathbf{c}_s \ . \quad (24)$$

The sample variance of $\mathbf{z}_s$ is estimated by

$$\hat{\sigma}^2_{\mathbf{z}_s} = \frac{1}{N_{pr}-1}\sum_{k=0}^{N_{pr}-1}(z_s[k] - \bar{z}_s)^2 \quad (25)$$

Under the assumption of uncorrelated noise between preamble symbols, var$\{z\}$ is obtained from

$$\text{var}\{z\} \approx N_{pr}\hat{\sigma}^2_{\mathbf{z}_s} \quad (26)$$

VI. Verification

A. Experimental Setup

The presented receiver architecture is tested in an indoor LOS office environment. The IEEE802.15.4a standard compliant signals are created by the transmitter shown in [9] and Fig. 2. The pulse sequence is generated by the multi-gigabit transceivers of an FPGA. The ternary signal is split into the positive and negative pulses of the signal. The positive and negative pulse sequences are then combined by a power combiner to the ternary signal. The pulses are shaped by a low pass filter for standard compliance and up-converted by a vector signal generator (VSG) to the carrier frequency f_c. The signal is finally bandpass filtered and transmitted via a UWB antenna.

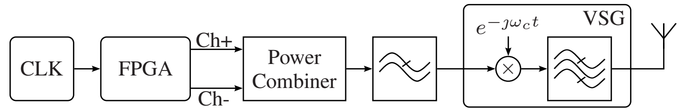

Fig. 2: Experimental transmitter setup

The receiver structure is depicted in Fig. 1. In the experimental setup, the signal is sampled and stored by an oscilloscope with 20 G-samples/s. Next, the digital part of the receiver is applied offline to the measurements, which allows flexible analysis of the parameters and algorithms. The carrier frequency f_c=4.4928 GHz, the pulse bandwidth is 499.2 MHz, the preamble code is number 6, $N_{pr} = 16$ and $L = 16$. The measurements were performed in an office LOS environment, where 72 measurements were taken within a range of 1 to 9 m.

B. Results

The experiments show the influence of noise in a typical application environment. The synchronization point is shifted to -15 ns (i.e., -5 m). This avoids confusing the detection of a strong noise component with the LOS path. The matched filter length is chosen to be 100 ns. Further, the measurement results are shifted by adding artificial noise to study the critical SNR region. Between one and 16 preamble symbols of the acquired signals have been analyzed to further increase the SNR range of the experimental data. Figs. 3(a) and 3(b) show the ranging results for the specific E_p/N_0 and LSNR values. The ranging performance of the thresholds c=$\{0.5, 0.6, 0.7\}$ is very similar in the sense of the working points. Thus, a threshold of c=0.6 has been chosen for this analysis. Fig. 3(a) shows the effect of averaging over 1, 4 and 16 preamble symbols. Clearly, averaging the preamble symbols 4 times increases the E_p/N_0 by 6 dB. It is observable at low SNRs, that the absolute distance error shows a uniform spread through about 5 meters. This boundary of 5m is based on the shift of the synchronization time by -15 ns. In these cases, a noise component is detected before the LOS component arrives. Within each measurement set for a given N_{pr}, the errors are not strongly correlated to the E_p/N_0 values, but a clear trend to an improved performance can be seen when more preamble symbols are used.

The LSNR takes directly the received pulse shape into account, see Fig. 3(b). The estimated distance error is almost always very low for high LSNR values. Further, the ranging algorithm is not able to detect the LOS component below an LSNR of approx. 3 dB. Excellent performance is obtained above 10 dB.

This is also observable in Fig. 4, where the probability of range estimations with an absolute distance error less than 1 m is plotted for specific SNRs. Note, that the threshold of 1 m has

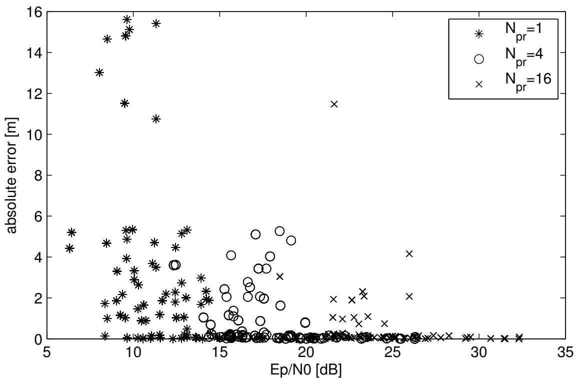

(a)

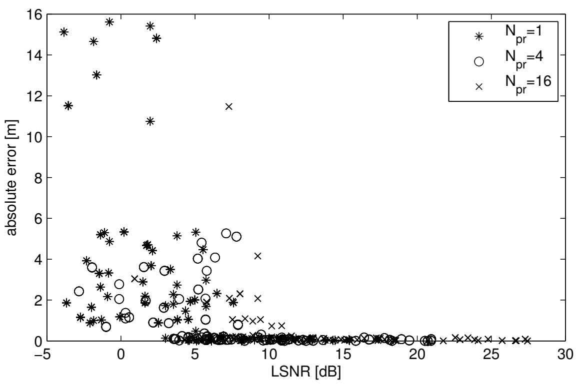

(b)

Fig. 3: Ranging results with a threshold $c = 0.6$ for specific (a) E_p/N_0 and (b) LSNR with respect to N_{pr} respectively.

been chosen, because the IEEE802.15.4a standard is designed to achieve a localization accuracy of better than 1m. To obtain this plot, the 72 measurements have been shifted by artificial noise to cover the range between -10 and +50 dB for each SNR. It is observable that the LSNR correlates best with the ranging performance. The transition zone LSNR between 20 and 80% is from 3.5 to 8.5 dB. The PSNR performs similarly, but needs a 2 dB higher SNR for 80% in comparison to the LSNR. For the E_p/N_0 value the SNR range spans from 10 to 23 dB, which shows that this performance metric is not very significant for ranging. But it will directly relate to the bit error rate (BER) performance for communications. For non-LOS channels, we expect an even higher discrepancy between the different performance metrics.

VII. Conclusions

This paper presents a coherent reference receiver for ranging in experimental setups. In the specific scenarios, the receiver can be used as a performance upper bound for less complex receiver architectures, e.g., non-coherent receivers. A signal model and statistical analysis of the receiver are given and a time-of-arrival ranging method is introduced. Several performance metrics are defined and analyzed for their suitability

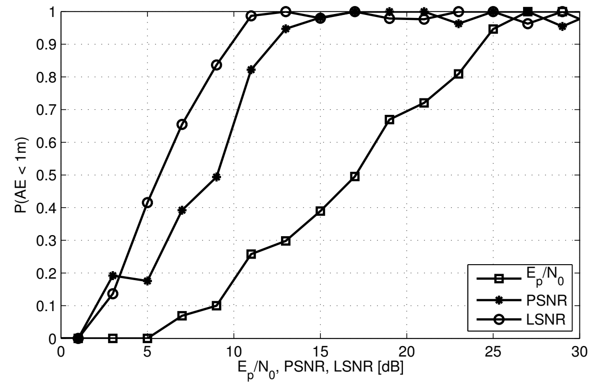

Fig. 4: Probability of an abs. distance error $< 1m$

for ranging. An indoor LOS measurement scenario is used to verify the receiver architecture with IEEE 802.15.4a compliant signals. E_p/N_0 shows quite low significance on the ranging experiments, but relates clearly to the BER performance of a matched filter receiver. The relevance of the Peak-Signal-to-Noise-Ratio (PSNR) and the Line-of-Sight Signal-to-Noise-Ratio (LSNR) for ranging is much higher. The working boundaries for this high performance receiver are experimentally determined in the ranging scenario.

Acknowledgment

The authors would like to thank C. F. Mecklenbraeuker, A. Adalan, and M. Fischer [9], Vienna University of Technology, for their support in the experiments. The project was partly funded by the Federal Ministry for Transport, Innovation and Technology (BMVIT) and the Austrian Research Promotion Agency (FFG).

References

[1] IEEE Working Group 802.15.4a, *Wireless Medium Access Control (MAC) and Physical Layer (PHY) Specifications for Low-Rate Wireless Personal Area Networks (WPANs)*, tech. rep. IEEE 2007

[2] K. Witrisal, *A Tutorial on Noncoherent UWB Systems*, Ch. 1 in Proc. Design and Analysis of Noncoherent UWB Transceivers, September 2008, Habilitation Thesis, Graz University of Technology, 2008

[3] I. Guvenc, Z. Sahinoglu, P.V. Orlik, *TOA Estimation for IR-UWB Systems With Different Transceiver Types* Microwave Theory and Techniques, IEEE Transactions on, 2006, Volume 54, pp. 1876-1886

[4] T. Gigl, G.J.M. Janssen, V. Dizdarevic, K. Witrisal, Z. Irahhauten, *Analysis of a UWB Indoor Positioning System Based on Received Signal Strength*, in Proc. 4th Workshop on Positioning, Navigation and Communication WPNC '07, 2007, pp. 97-101

[5] T. Gigl, J. Preishuber-Pfluegl, K. Witrisal, *Statistical Analysis of a UWB Energy Detector for Ranging in IEEE 802.15.4a*, Ultra-Wideband, 2009. ICU 2009. IEEE International Conference on,

[6] V. Dizdarevic, K. Witrisal, *Statistical UWB Range Error Model for the Threshold Leading Edge Detector*, in Proc. 6th International Conference on Information, Communications & Signal Processing, 2007, pp. 1-5

[7] I. Guvenc, Z. Sahinoglu, *Threshold-Based TOA Estimation for Impulse Radio UWB Systems*, Ultra-Wideband, 2005. ICU 2005. IEEE International Conference on, 2005, pp. 420-425

[8] J. G. Proakis, M. Salehi *Communication Systems Engineering - Second Edition*, Prentice Hall 2002

[9] A. Adalan, M. Fischer, T. Gigl, K. Witrisal, A.L. Scholtz, C.F. Mecklenbraeuker, *Ultra-Wideband Radio Pulse Shaping Filter Design for IEEE802.15.4a Transmitter*, in Proc. Wireless Communications & Networking Conference, WCNC 2009